Elio J. König, ^{1,2} Yashar Komijani, ^{3,2} and Piers Coleman^{2,4}

¹Max-Planck-Institut für Festkörperforschung, 70569 Stuttgart, Germany
²Department of Physics and Astronomy, Center for Materials Theory,
Rutgers University, Piscataway, NJ 08854, USA
³Department of Physics, University of Cincinnati, Cincinnati, OH 45221, USA
⁴Department of Physics, Royal Holloway, University of London, Egham, Surrey TW20 0EX, UK
(Dated: January 24, 2022)

We develop a quantum spin liquid theory for quantum magnets with easy-plane ferromagnetic exchange. These strongly entangled quantum states are obtained by dimer coverings of 2D lattices with triplet $S=1, m_z=0$ bonds, forming a triplet resonating valence bond (tRVB) state. We discuss the conditions and the procedure to transfer well-known results from conventional singlet resonating valence bond theory to tRVB. Additionally, we present mean field theories of Abrikosov fermions on 2D triangular and square lattices, which can be controlled in an appropriate large N limit. We also incorporate the effect of charge doping which stabilizes p+ip-wave superconductivity. Beyond the pure theoretical interest, our study may help to resolve contradictory statements on certain transition metal chalcogenides, including 1T-TaS₂, 1T-TaSe₂, as well as CrSiTe₃ and CrGeTe₃.

I. INTRODUCTION

A. Resonating Valence Bond theory

Resonating valence bond (RVB) theory describes prototypical quantum spin liquid (QSL) states which were originally proposed by Anderson^{1,2} for the 2D Heisenberg antiferromagnet on a triangular lattice. The frustrated magnetic interactions entangle spins on different sites of the lattice in a pairwise fashion into singlet valence bonds. When the system resonates between a multitude of degenerate bond configurations, the RVB state forms a quantum superposition of a macroscopic number of wave functions. RVB states with short range bonds on two dimensional lattices do not break any of the system's symmetries and satisfy modern criteria^{3,4} for a quantum spin liquid (QSL) as a highly entangled state with topological order. ⁵ While it is now known that the ground state of the nearest neighbor Heisenberg antiferromagnet on the triangular lattice is not a QSL state, numerical studies suggest that QSL behavior can be stabilized by next nearest neighbor interactions. 6-8 Short range RVB states are furthermore known to be the exact ground state of dimer models⁹ and even of appropriately designed SU(2) invariant spin Hamiltonians 10 with n-spin interactions (including n > 2).

In addition to its progenitorial role in the study of QSLs, RVB theory is also quintessential for superconductivity beyond the BCS paradigm. Specifically in the context of cuprate superconductors, preentangled singlet bonds are believed to constitute a pair condensate which turns into a bona fide superconductor as doping liberates the charge degrees of freedom from a correlated Mott insulator. ¹¹ As a major advantage over other approaches, RVB theory ^{12,13} and related gauge theories ^{14,15} naturally account for pseudogap phenomena ¹⁶ in an elegant and economical fashion.

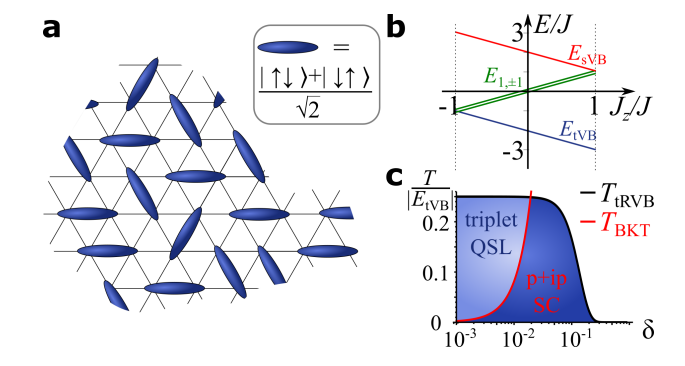


FIG. 1. a Illustration of a dimer covering of the triangular lattice with nearest neighbor triplet bonds (see inset for definition of a dimer). The tRVB ground state is a superposition of such coverings and a triplet quantum spin liquid (QSL). b Energy levels of a pair of spins with anisotropic interaction as in Eq. (6), illustrating that the triplet valence bond (tVB) is lowest in energy. c Finite temperature mean field phase diagram for the model introduced in Eq. (10) as a function of temperature and hole doping δ . A p+ip superconductor (SC) appears by doping the QSL. For this plot, we used $|E_{\rm tVB}|/t=0.1$.

B. Spin liquid candidates with ferromagnetic correlations

The experimental search for QSL materials has lately enjoyed increased attention. Here, we concentrate on the proposal that the layered van-der-Waals material 1T-TaS $_2$ and related compounds 1T-NbS $_2$ and 1T-TaS $_2$, may form a 2D QSL on a triangular lattice ^{17,18}, while the 2D ferromagnets CrXTe $_3$ with X=Si,Ge may display 2D QSL behavior on a honeycomb lattice above T_{Curie}.

When 1T-TaS₂ is cooled below 200K, a peculiar CDW order rearranges the atoms of a plane into a triangular superlattice where 13 Ta atoms per unit cell form a star-of-David structure (for a recent STM visualization, see e.g. 19). As each of the Ta atoms contributes

one 5d electron, twelve electrons fill 6 emergent bands and leave an emergent Hubbard model with one electron per supercell behind. Mott localization is generally accepted in view of disorder-dependent activated behavior below $T \sim 50K^{20-22}$ and the observation of Hubbard bands. 19,23 A transition displaying magnetic ordering is ruled out down to temperatures as low as 20mK by μ SR and susceptibility measurements. ^{18,21,24} The ground-state is a paramagnet with a substantial. temperature independent magnetic susceptibility χ , with a small Curie-Weiss upturn, likely the result of disorder^{18,21}. These observations raise the fascinating possibility that this system forms a QSL, a paramagnetic spin state with a characteristic temperature (set by the spin-spin interaction energy $J)^{17}$. Support for this interpretation derives from the recent observation of a finite Sommerfeld coefficient $\gamma = C_V/T$ in the specific heat ^{21,22} and a linear temperature dependence in the thermal conductivity ²², features that are consistent with the formation of a QSL with a spinon-Fermi surface. Moreover, the Wilson ratio χ/γ between the susceptibility and Sommerfeld coefficient lies in a range that is compatible with weakly interacting spinons. A similar phenomenology and evidence for QSL behavior was recently observed in tunneling experiments on monolayer 1T-TaSe₂.²⁵

Despite this interesting experimental development, we are not aware of a microscopic theory which explains the large spin-interaction scale J required to account for the temperature independent susceptibility. Both a heuristic approach of decoupled star-of-David clusters²⁶ and density functional theory²⁷ suggest an in-plane hopping strength $t \sim 10 meV$, which taken together with a realistic $U \sim 200 meV$ implies an antiferromagnetic superexchange interaction $J \sim +5K$. Moreover, several abinitio studies of 1T-TaS₂ and phenomenologically similar monolayer 1T-NbSe₂, 1T-TaSe₂ predict a ferromagnetic ground state^{27–30} with exchange constant $J \sim -5K$ and a few percent anisotropy which favors alignment in the basal plane. ^{28,31} Leaving the conundrum of the smallness of |J| to future studies, the apparent controversy on the sign of J motivates us to pose the fundamental and fascinating question, whether a quantum spin-liquid can exist in presence of ferromagnetic interactions. Specifically, we concentrate on the easy-plane scenario, which could be induced by the prominent role attributed to the spin-orbit interaction due to the heavy Ta atoms. 32 On the basis of an affirmative answer, we further study the effect of doping away from the Mott limit and discover a time-reversal symmetry breaking (TRSB) p + ip-wave superconductor. This is particularly interesting in light of the recent discovery of TRSB superconductivity in 4H-TaS₂ (in which monolayers of 1T-TaS₂ are alternatingly stacked with metallic 1H-TaS₂ monolayers). ³³

Another potential candidate for a tRVB state is $CrXTe_3$ with X=Si, Ge, previously referred to as 2D ferromagnetic semiconductors. These are layered system with Cr^{3+} ions on a honeycomb lattice. In the case of $CrSiTe_3$, transport measurements indicate a thermally

activated mechanism with an indirect bulk gap of around 0.4eV, consistent with optical measurement. There is a bulk Curie temperature of around 33K, often accompanied by a structural transition, ³⁴ which is enhanced to 80K in the case of monolayer. ^{35,36} The origin of the insulating phase at higher temperature is noteworthy: The local crystalline structure of the material splits the levels of the d-shell whose orbitals are half-filled at the Fermi level. The narrow bandwidth of d-orbitals strongly enhances the correlations between electrons, ³⁷ leading to a Mott insulator in contrast to the predictions of ab initio calculations. 38 The fact that the Curie temperate is less than the gap indicates that this is a local-moment system with a saturated magnetic moment of $3\mu_B/\text{Cr}$. The ferromagentism between Cr electrons is induced by the super-exchange via Te sites³⁷ which dominates over a direct anti-ferromagnetic super-exchange. Nonetheless, there are anti-ferromagnetic inter-layer correlations, which seem to be responsible for reducing the Curie temperature in the bulk compared to the monolayer. While there is a slight Ising anisotropy in the transition temperature, significant short-range in-plane magnetic correlations persists all the way up to 150K. 39 Under pressure the system becomes metallic and, after a structural transition at P~9GPa, it turns superconducting with a T_c of around 4K⁴⁰ which is relatively independent of pressure up to around 50GPa. Based on this, we propose that this material is a potential candidate for the tRVB physics and the associated superconductivity upon doping which is discussed in this paper.

C. RVB theory vs. triplet RVB theory

In the past, QSL theories with *Ising* interactions (e.g. the Kitaev model⁴¹) were discussed both for ferromagnetic and antiferromagnetic interactions. Here, we develop the concept QSLs with ferromagnetic easy plane interactions, leading to the concept of triplet resonating valence bonds (tRVB). This idea was recently proposed to account for the observation of strange metal behavior near a ferromagnetic quantum critical point in the heavyfermion material CeRh₆Ge₄. ⁴² It was subsequently proposed that such a tRVB quantum material can be a parent state for triplet superconductivity in Hund's metals, and in particular in Iron-based superconductors. ^{43,44} As we will now explain, the underlying principles of tRVB theory parallel Anderson's RVB theory. The basic building block of the RVB theory, is a singlet valence bond (sVB), formed between two spins at sites i and j

$$|[i,j]\rangle = \frac{|\uparrow_i\rangle |\downarrow_j\rangle - |\downarrow_i\rangle |\uparrow\rangle_j}{\sqrt{2}},\tag{1}$$

where the notation [i,j] = -[j,i] is used to reflect the antisymmetry under spin exchange. This state is the ground state of a two-site Hamiltonian with antiferro-

magnetic spin-spin interaction

$$H_{\text{SVB}} = J\vec{\sigma}_i \cdot \vec{\sigma}_i. \tag{2}$$

Here, $\sigma_{x,y,z}$ are Pauli Matrices and $\hbar=1$ throughout the paper. In a lattice of spins that interact antiferromagnetically, such bonds can develop between any pairs of spin, forming the state

$$|P_s\rangle = \prod_{[i,j]\in P} |[i,j]\rangle$$
 (3)

where P is a particular choice of pairs of spins. In a lattice, competition between antiferromagnetic spin interactions cause such a state to resonate between different configurations $|P_s\rangle$, forming a quantum-mechanical admixture of all such states, a resonating valence bond state

$$|\text{RVB}\rangle = \sum_{P} A_P |P_s\rangle.$$
 (4)

The simplest example of such a state is the short-range RVB state, formed from the quantum superposition of all possible coverings with nearest neighbor sVB dimers.

By contrast, the basic building block for tRVB theory is a triplet valence bond (tVB)

$$|(i,j)\rangle = \frac{|\uparrow_i\rangle|\downarrow_j\rangle + |\downarrow_i\rangle|\uparrow\rangle_j}{\sqrt{2}}.$$
 (5)

This entangled state is the ground state of a two-site Hamiltonian with easy plane ferromagnetic spin-spin interaction

$$H_{\text{tVB}} = -J[\sigma_{x,i}\sigma_{x,j} + \sigma_{y,i}\sigma_{y,j}] + J_z\sigma_{z,i}\sigma_{z,j}, \qquad (6)$$

with $J_z > -J, J > 0$, Fig. 1 b. In analogy to RVB, the tRVB state on a lattice is the macroscopic superposition

$$|\text{tRVB}\rangle = \sum_{P} A_{P} |P_{t}\rangle$$
 (7)

of states

$$|P_t\rangle = \prod_{(i,j)\in P} |(i,j)\rangle \tag{8}$$

corresponding to a particular tiling of triplet valence bonds. Crucially, the singlet and triplet valence bonds $|sVB\rangle$, $|tVB\rangle$ both form Bell pairs and are therefore suitable for the construction of highly entangled QSL states, Fig. 1 a.

The case where $J_z = J$ is of particular interest, because in this case H_{tVB} is a unitary transformation of H_{VB} obtained by rotating the spin at site j through 180° about the z axis, i.e $H_{\text{tVB}} = \sigma_{z,j} H_{\text{sVB}} \sigma_{z,j}$. Consequently, for a bipartite lattice with only intersublattice valence bonds, the tRVB and RVB wave functions are related by a unitary transformation obtained by a 180° rotation of spins on one sublattice. Importantly, this implies that nearest neighbor tRVB states on the 2D square lattice are quantum spin-liquids with short range spin correlators, Fig. 2, while nearest neighbor tRVB states on the 3D cubic lattice display long range order in $\langle \sigma_{x,i}\sigma_{x,j} \rangle$, $\langle \sigma_{y,i}\sigma_{y,j} \rangle$ and $(-1)^{i+j}\langle \sigma_{z,i}\sigma_{z,j} \rangle$ (i,j are site indices). Moreover, the properties of RVB states which are obtained from quantum dimer models, including the topological ground state degeneracy for the 2D triangular lattice are independent on whether a given dimer represents a singlet or triplet bond. On this basis we conclude that nearest neighbor tRVB theory is a gapped \mathbb{Z}_2 spin liquid on the 2D triangular lattice.

Using these parallels, we here present the first field-theoretical (fractionalized) tRVB theory. We fractionalize the electrons into Abrikosov pseudofermions and slave bosons, 49 and derive a mean field theory of tRVB which is analogous to the mean field approach to the RVB state. 12,50 Our study particularly focuses on non-bipartite lattices and on the impact of charge doping, because in these two cases the unitary mapping between RVB and tRVB theory breaks down. Most importantly, we thereby develop a formalism for entanglement driven triplet superconductivity: Just as an RVB state may be considered as a Gutzwiller projection (denoted $\hat{P}_{\rm G}$) of singlet d-wave superconductive state, i.e.

$$|\text{RVB}\rangle = \hat{P}_{\text{G}} |\text{BCS}: d_{x^2 - y^2}\rangle,$$
 (9a)

the tRVB states considered here are Gutzwiller projected triplet $p_x + ip_y$ states,

$$|\text{tRVB}\rangle = \hat{P}_{G} |\text{BCS:} p_x + i p_y\rangle.$$
 (9b)

At half-filling, both RVB and tRVB theories describe an insulator, yet, upon hole-doping, pre-entangled Cooper pairs get liberated and form a superconducting phase.

D. Outline

The rest of the paper is structured as follows: In Sec. II we introduce a t-J model for an anisotropic quantum ferromagnet and the formalism of fractionalization. In Sec. III we present a discussion of homogeneous mean field solutions, both in the Mott limit and upon charge doping. We conclude with an outlook, Sec. IV. Three appendices contain details: Appendix A contains technicalities on the free energy expansion, in Appendix B we demonstrate that an appropriately designed large N limit can stabilize the tRVB mean field solution, while Appendix C contains details on the Berezinskii-Kosterlitz-Thouless transition establishing a 2D holon superfluid.

II. XXZ FERROMAGNET: MODEL AND FORMALISM

In this section we introduce model and formalism using the following 2D t-J model with XXZ easy plane ferromagnetic interactions

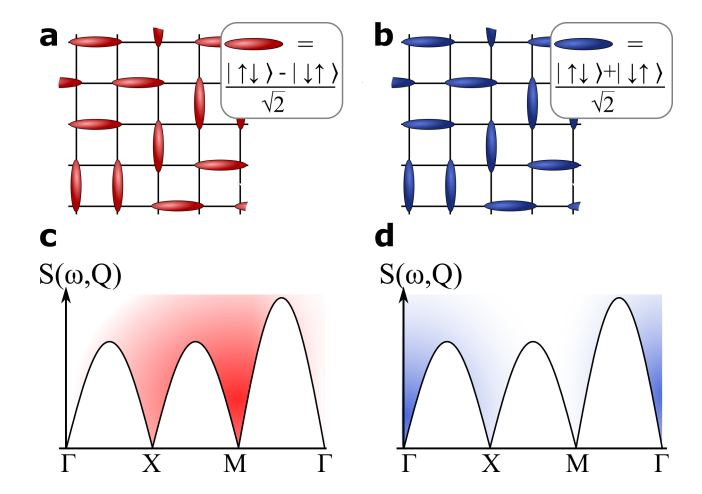


FIG. 2. The application of a 180° spin rotation on one sublattice, $\vec{\sigma}_j \to \sigma_{z,j} \vec{\sigma}_j \sigma_{z,j}$, transforms a nearest neighbor RVB state on the square lattice (panel a) into a nearest neighbor tRVB state (panel b). By consequence, the dynamical structure factor $S(\omega, \mathbf{Q}) = \sum_i \int dt e^{i\omega t - \mathbf{x}_i \cdot \mathbf{Q}} \langle \sigma_{+,i}(t) \sigma_{-,0}(0) \rangle$, $\sigma_{\pm} = [\sigma_x \pm i\sigma_y]/2$, of the tRVB state (schematic, panel d) is shifted by (π, π) as compared to the RVB state (panel c).

$$H = -t \sum_{\langle i,j \rangle, \sigma} [X_{\sigma 0}^{(i)} X_{0\sigma}^{(j)} + H.c.] - \mu \sum_{i,\sigma} X_{\sigma \sigma}^{(i)}$$
$$- J \sum_{\langle i,j \rangle} {\{\hat{\sigma}_{x}^{(i)} \hat{\sigma}_{x}^{(j)} + \hat{\sigma}_{y}^{(i)} \hat{\sigma}_{y}^{(j)}\}}$$
$$+ J_{z} \sum_{\langle i,j \rangle} \hat{\sigma}_{z}^{(i)} \hat{\sigma}_{z}^{(j)} + V \sum_{\langle i,j \rangle} [\sum_{\sigma} X_{\sigma \sigma}^{(i)}] [\sum_{\sigma} X_{\sigma \sigma}^{(j)}] \}. (10)$$

The Hubbard operators $X_{0\sigma}^{(i)} = |0\rangle_i \langle \sigma|_i$, and $X_{\sigma'\sigma}^{(i)} = |\sigma'\rangle_i \langle \sigma|_i$ satisfy the standard Hubbard superalgebra (see, e.g., Ref 51). The spin operator is $\hat{\sigma}_{\mu} = \sum_{\sigma\sigma'} [\sigma_{\mu}]_{\sigma\sigma'} X_{\sigma\sigma'}$. For a given pair of spins, the singlet state $(|\uparrow\downarrow\rangle - |\downarrow\uparrow\rangle)/\sqrt{2}$ has energy $E_{\text{sVB}} = 2J - J_z$, the triplet states $|\uparrow\uparrow\rangle, |\downarrow\downarrow\rangle$ have energy $E_{1,\pm 1} = J_z$ and the $S = 1, m_z = 0$ state $(|\uparrow\downarrow\rangle + |\downarrow\uparrow\rangle)/\sqrt{2}$ has energy $E_{\text{tVB}} = -2J - J_z$, see Fig. 1 b. The energy scale E_{tVB} of these triplet valence bonds (tVBs) will be crucial throughout the paper, it is manifest that for an easy plane ferromagnet (defined by $J_z > -J$) the ground state of a pair of spins is given by the tVB. We consider both triangular and square lattices.

A. Slave-Boson representation

We follow the standard slave boson representation⁵¹ $X_{\sigma 0}^{(i)} = f_{i,\sigma}^{\dagger} b_i, X_{\sigma \sigma'}^{(i)} = f_{i,\sigma}^{\dagger} f_{i,\sigma'}, X_{00}^{(i)} = b_i^{\dagger} b_i$ with the local constraint $b_i^{\dagger} b_i + \sum_{\sigma} f_{i,\sigma}^{\dagger} f_{i,\sigma} = 1$. With a slight abuse of language (see details below), we call $f_{i\sigma}$ a spinon and b_i a holon.

The corresponding Hamiltonian is

$$H = \sum_{\langle i,j \rangle} \left[-t (f_i^{\dagger} b_i b_j^{\dagger} f_j + H.c.) + J_z (f_i^{\dagger} \sigma_z f_i) (f_j^{\dagger} \sigma_z f_j) \right.$$
$$-J \sum_{\mu=x,y} (f_i^{\dagger} \sigma_{\mu} f_i) (f_j^{\dagger} \sigma_{\mu} f_j) + V b_i b_i^{\dagger} b_j b_j^{\dagger} \right]$$
$$+ \sum_{i} \left[\lambda_i (f_i^{\dagger} f_i + b_i^{\dagger} b_i - 1) - \mu b_i b_i^{\dagger} \right]. \tag{11}$$

We have added a Lagrange multiplier λ_i to enforce the local constraint and employ a spinor notation $f_i = (f_{i,\uparrow}, f_{i,\downarrow})^T$. So far, no approximations were made, Eq. (10) was merely rewritten.

As usual, a number of subtleties follow from the prefractionalized construction. The local nature of the constraints leads to the emergence of a compact U(1) gauge theory (generated by local rotations $f_{i,\sigma} \to e^{i\phi_i} f_{i,\sigma}, b_i \to$ $e^{i\phi_i} b_i$). Depending on whether the U(1) gauge theory is deconfining or confining, a quantum spin liquid with well defined (deconfined) spinons, is or is not realized. ⁵²

It is well known that 2D compact U(1) gauge theories without matter fields are confining due to a proliferations of monopoles. 53 While at first sight, this suggests that a truly fractionalized state can not develop from Eq. (11), there are essentially three ways to avoid confinement: First, the spinons form a time reversal symmetry broken insulator which leads to the addition of a Chern-Simons term to the gauge theory. Second, the spinons may form a superconductor, and thereby spontaneously "break" the symmetry to \mathbb{Z}_2 (\mathbb{Z}_2 gauge theories are known to allow for deconfinement in 2D. 54) In this context, we mention that generically the physical spinons and the $f_{i,\sigma}$ are related but not the same. ⁵⁵ Third, when the spinons remain gapless an infinite number of degrees of freedom⁵⁶ can suppress the proliferation of monopole operators and thereby annihilate the confining effect.

In this paper, which is the first on fractionalization in tRVB theory, we will not study gauge field fluctuations. Instead, we here derive mean field solutions of the spinon Hamiltonian. However, we emphasize that these solutions are superconducting and time reversal symmetry breaking. It is therefore reasonable to expect the possibility of deconfinement in the gauge sector.

B. Reminder of slave-boson theory for RVB

Before developing the slave-boson theory of tRVB, it appears beneficial to remind the reader about the analogous formalism for conventional RVB. ^{12,57,58} We mostly follow Kotliar and Liu¹² and consider the conventional t-J model on the square lattice

$$H = -t \sum_{\langle i,j \rangle, \sigma} [X_{\sigma 0}^{(i)} X_{0\sigma}^{(j)} + H.c.] - \mu \sum_{i,\sigma} X_{\sigma \sigma}^{(i)} + J \sum_{\langle i,j \rangle} \{\hat{\hat{\sigma}}^{(i)} \cdot \hat{\hat{\sigma}}^{(j)} + V \sum_{\langle i,j \rangle} [\sum_{\sigma} X_{\sigma \sigma}^{(i)}] [\sum_{\sigma} X_{\sigma \sigma}^{(j)}] \}, (12)$$

which in slave boson formalism may be written as

$$H = \sum_{\langle i,j \rangle} \left[-t(f_i^{\dagger} b_i b_j^{\dagger} f_j + H.c.) + J(f_i^{\dagger} \vec{\sigma} f_i) \cdot (f_j^{\dagger} \vec{\sigma} f_j) + V b_i b_i^{\dagger} b_j b_j^{\dagger} \right] + \sum_i \left[\lambda_i (f_i^{\dagger} f_i + b_i^{\dagger} b_i - 1) - \mu b_i b_i^{\dagger} \right].$$
(13)

The RVB theory summarized in Eq. (12) and (13) parallels the tRVB theory exposed in Eq. (10) and Eq. (11). Specifically, the interaction part of Eq. (10) at $J_z = J$ is obtained from Eq. (12) by applying a unitary transformation $\hat{\sigma} \to \hat{\sigma}_z \hat{\sigma} \hat{\sigma}_z$ on every other site. As a direct consequence, spinon interactions in the slave-boson formulation, Eq. (11) follow from Eq. (13) by applying the transformation $f_j \to (\sigma_z)^j f_j$ on every second site. However, at $t \neq 0$, tRVB theory is not related to RVB theory by a mere unitary transformation, because $t(f_i^{\dagger}b_ib_j^{\dagger}f_j) \to t(f_i^{\dagger}\sigma_z b_ib_j^{\dagger}f_j)$ leads to a spin-dependent sign of the hopping.

One may decouple the spinon-interaction of Eq. (13) as follows 12

$$H = -t \sum_{\langle i,j \rangle, \sigma} [f_{i,\sigma}^{\dagger} b_i b_j^{\dagger} f_{j,\sigma} + H.c.]$$

$$+ \sum_{i} [\lambda_i (\sum_{\sigma} f_{i,\sigma}^{\dagger} f_{i,\sigma} + b_i^{\dagger} b_i - 1) - \mu b_i b_i^{\dagger}]$$

$$- \sum_{\langle i,j \rangle} \{ (\kappa_{ij} f_i^{\dagger} f_j + H.c.) - [\Delta_{ij} f_i^T (i\sigma_y) f_j + H.c.] \}$$

$$+ \frac{2}{|E_{\text{AFM}}|} \sum_{\langle i,j \rangle} [|\kappa_{ij}|^2 + |\Delta_{ij}|^2] + V \sum_{\langle i,j \rangle} b_i b_i^{\dagger} b_j b_j^{\dagger}, \quad (14)$$

where $E_{\rm AFM} = -3J$ is the energy of a single sVB for isotropic antiferromagnetic interactions. As first discussed by Affleck, Zou, Hsu and Anderson, ⁵⁹ at half-filling, the model displays an SU(2) symmetry in Nambu space. This is traditionally represented using Nambu spinors $\psi_{i,\sigma} = (f_{i,\sigma}, (i\sigma_y)_{\sigma\sigma'} f_{i,\sigma'}^{\dagger})^T$, the matrix

$$U_{ij} = \begin{pmatrix} \kappa_{ij} & \Delta_{ij} \\ \Delta_{ij}^* & -\kappa_{ij}^* \end{pmatrix}$$
 (15)

and the identification

$$-\left[\kappa_{ij}f_i^{\dagger}f_j - \Delta_{ij}f_i^T(i\sigma_y)f_j + H.c.\right] + 2\frac{|\kappa_{ij}|^2 + |\Delta_{ij}|^2}{|E_{AFM}|}$$
$$= -\psi_i^{\dagger}U_{ij}\psi_j + \frac{\operatorname{tr}[U_{ij}^{\dagger}U_{ij}]}{|E_{AFM}|}.$$
 (16)

The symmetry is given by an SU(2) rotation in Nambu space, $\psi_i \to W_i \psi_i, U_{ij} \to W_i U_{ij} W_j$. We equivalently represent this symmetry in the notation $U_{ij} = i\kappa''_{ij} + \vec{u}_{ij} \cdot \vec{\tau}$ as an SO(3) rotation of the vector of order parameters on a given link

$$\vec{u}_{ij} = (\Delta'_{ij}, \Delta''_{ij}, \kappa'_{ij}), \tag{17}$$

where $\text{Re}[\Delta_{ij}] = \Delta'_{ij}$, $\text{Im}[\Delta_{ij}] = \Delta''_{ij}$ and analogously for κ_{ij} .

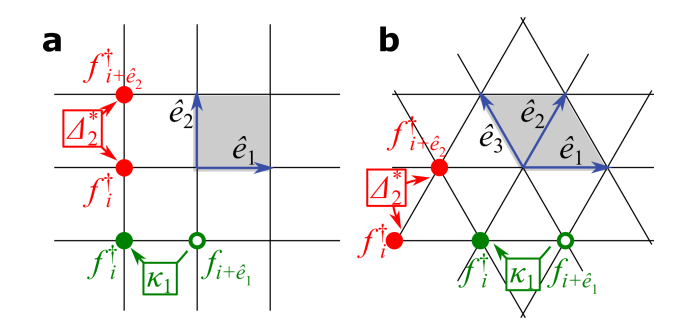


FIG. 3. Convention of unit vectors \hat{e}_l ($l=1,\ldots,z/2$) and illustration of mean field parameters on square and triangular lattices. The homogeneous mean-field solutions discussed in this paper correspond to associating complex hopping κ_l and pairing Δ_l amplitudes to each of the z/2 links of each unit cell (which is shaded gray).

Kotliar and Liu¹² considered mean field solutions of Eq. (14) under the simplifying assumption of translational invariance, i.e. $\lambda_i = \lambda$, $\kappa_{ij} = \kappa_1$ ($\kappa_{ij} = \kappa_2$) on all horizontal (vertical) links and analogously for Δ_{ij} . Thus, $\kappa_{1,2}$ corresponds to a complex hopping amplitude and $\Delta_{1,2}$ to an intersite pairing gap on a given link, see Fig. 3 a. In the absence of doping, the ground state manifold of energetically equivalent solutions is characterized by the condition $\vec{u}_1 \cdot \vec{u}_2 = 0$ (i.e. $\vec{u}_1 \propto (1,0,0)$ and $\vec{u}_2 \propto (0,1,0)$ and SO(3) rotations theoreof). However, doping adds a linear symmetry breaking field to the free energy, $\delta F_{\text{RVB}} \propto -\delta(0,0,1) \cdot [\vec{u}_1 + \vec{u}_2]$, such that the manifold of mean field solutions is reduced to d-wave superconducting solutions, i.e. $\vec{u}_1 \propto (1,0,1), \vec{u}_2 \propto (-1,0,1)$ or equivalent solutions obtained by O(2) rotations along the axis (0, 0, 1).

Finally, a physical superconductor is reached when both the spinons and the bosons form a superfluid.

C. Hubbard-Stratonovich decoupling

After having reviewed conventional RVB theory, we return to the model of interest in the tRVB context, Eqs. (10), (11). We decouple the interaction in the two channels of strongest nearest neighbor attraction

$$H = -t \sum_{\langle i,j \rangle, \sigma} \left[f_{i,\sigma}^{\dagger} b_i b_j^{\dagger} f_{j,\sigma} + H.c. \right]$$

$$+ \sum_{i} \left[\lambda_i \left(\sum_{\sigma} f_{i,\sigma}^{\dagger} f_{i,\sigma} + b_i^{\dagger} b_i - 1 \right) - \mu b_i b_i^{\dagger} \right]$$

$$- \sum_{\langle i,j \rangle} \left\{ \left(\kappa_{ij} f_i^{\dagger} \sigma_z f_j + H.c. \right) + \left[\Delta_{ij} f_i^T (i\sigma_y) \sigma_z f_j + H.c. \right] \right\}$$

$$+ \frac{2}{|E_{\text{tVB}}|} \sum_{\langle i,j \rangle} \left[|\kappa_{ij}|^2 + |\Delta_{ij}|^2 \right] + V \sum_{\langle i,j \rangle} b_i b_i^{\dagger} b_j b_j^{\dagger}. \tag{18}$$

The σ_z matrices in the third line appear for triangular and square lattices alike, in the latter case they directly follow from Eq. (14) by virtue of the transformation $f_j \to (\sigma_z)^j f_j$. The logic for decoupling particle-hole and

particle-particle channels simultaneously is motivated as follows: In the field integral, we can discriminate particleparticle and particle hole channel from the structure in frequency space: $f_{\epsilon_1,\sigma_1}^{\dagger} f_{\epsilon_2,\sigma_2} f_{\epsilon_3,\sigma_3}^{\dagger} f_{\epsilon_4,\sigma_4} \delta_{\epsilon_1+\epsilon_3-\epsilon_2-\epsilon_4}$ has three different channels, according to which of the frequencies $\epsilon_{1,2,3,4}$ are closeby in magnitude. We keep all attractive channels, while the repulsive channels will be dropped.

The procedure of decoupling nearest neighbor channels whilst disregarding onsite (magnetic) order parameters is controlled in appropriately designed large N limits (in the present XXZ case of the Sp(2N) group). Extrapolating these calculations to SU(2) = Sp(2) is uncontrolled, even though historically grown. 12 In particular, the procedure misses all magnetically ordered phases, e.g. ferromagnetism, to which we compare heuristically in appropriate sections of the main part of this paper.

We included a controlled Sp(2N) treatment for the insulating limit in App. B - this demonstrates that the mean field triplet QSL solutions presented here are the ground state of the Hamiltonian (11) in a well defined limit. For the sake of physical clarity, we consider the formally uncontrolled spin-1/2 system in the main text, and emphasize that we leave the search for spin-1/2 Hamiltonians with rigorous tRVB ground states to the future. This strategy parallels the early development of singlet RVB theory, ^{1,12,50} which predated modern, numerically exact, QSL studies, e.g. for antiferromagnetic models on the triangular lattice $^{6-8,26}$, by more than three decades.

HOMOGENEOUS MEAN FIELD SOLUTIONS

We here focus on the simplest case of uniform mean field solutions (note that this excludes certain π flux solutions 50,60) of Eq. (18). We treat the constraint on average (considering λ a constant chemical potential) and use a mean field decoupling of the hopping term, by replacing $t\langle b_i b_i^{\dagger} \rangle \to t_f$ and $\sum_{\sigma} t\langle f_i^{\dagger} f_i \rangle \to t_b$ in Eq. (18), i.e.

$$tf_{i,\sigma}^{\dagger}b_ib_i^{\dagger}f_{j,\sigma} \to t_f f_{i,\sigma}^{\dagger}f_{i,\sigma} + t_b b_i b_i^{\dagger} - t_f t_b/t. \tag{19}$$

We will discuss the self-consistency of this replacement in Sec. IIIF, and for the moment we concentrate on the fermionic part of the Hamiltonian.

Square lattice

We first discuss the situation on the square lattice, where the order parameters are $\Delta_{1,2}, \kappa_{1,2}$ (the value on vertical and horizontal links may differ) and λ (as determined by the average occupation $1 - \delta$). The spinon Hamiltonian in Nambu and momentum space is ($\psi_{\mathbf{k}}$ = $(f_{\mathbf{k}}^T, f_{-\mathbf{k}}^{\dagger}(-i\sigma_y))^T)$

$$H_f = \frac{1}{2} \sum_{\mathbf{k}} \psi_{\mathbf{k}}^{\dagger} h(\mathbf{k}) \psi_{\mathbf{k}}.$$
 (20a)

It is convenient to express the spinon Hamiltonian $h(\mathbf{k})$ using Pauli matrices $\vec{\tau}$ in Nambu space and the notation $\vec{u}_l = (\Delta_l', \Delta_l'', \kappa_l'')$

$$h(\mathbf{k}) = \xi_{\mathbf{k}} \tau_z - 2 \sum_{l=1}^{z/2} \sigma_z \left[\kappa_l' \cos(\mathbf{k} \cdot \hat{e}_l) - \vec{u}_l \cdot \vec{\tau} \sin(\mathbf{k} \cdot \hat{e}_l) \right].$$
(20)

In this notation, the previously mentioned⁵⁹ emergent SU(2) symmetry in Nambu space is manifest in the case $\xi_{\mathbf{k}} = 0$. We introduced $\xi_{\mathbf{k}} = -2t_f \sum_{l=1}^{z/2} \cos(\mathbf{k} \cdot \hat{e}_l) + \lambda$ as well as the basis vectors $\hat{e}_1 = (1, 0)^T$, $\hat{e}_2 = (0, 1)^T$, see Fig. 3 a), z = 4 is the coordination number. We use the shorthand notation $k_l = \mathbf{k} \cdot \hat{e}_l$ in the following.

We next evaluate the ground state energy for several trial solutions at $\delta = 0$, see Tab. I, left column.

First, we consider normal state solutions, the simplest of which is $\kappa_1'=\kappa_2'>0, \; \vec{u}_l=0$ (the sign of the hopping can be chosen at will, as spin-up and spin-down spinons have reversed dispersion). This state displays a spinon Fermi surface, C_4 symmetry and $\lambda = 0$ corresponds to half filling. The fermionic contribution to the ground state energy is $E_f = -C\kappa'_l$ with $C \approx -1.62$. The mean field energy per site is obtain by optimizing $E = E_f +$ $z\kappa_I^{\prime 2}/|E_{\text{tVB}}|$ from which we obtain $E = -|E_{\text{tVB}}|C^2/(4z)$, as quoted in Tab. I. (An analogous procedure is used for all of the following states, only the numerical value of \mathcal{C} changes from case to case).

As a second normal state solution we consider $\kappa_1'' = \kappa_2'' > 0$, while all other parameters $\kappa_l' = \Delta_l' = \Delta_l'' = 0$. For the square lattice the total enclosed flux per square vanishing ishes for homogeneous imaginary hopping $\kappa_l'' > 0$, thus this solution is gauge equivalent to the previously discussed solution with real hopping (we will see in the next section that such an equivalence does not hold for analogous two states on the triangular lattice).

Finally, we consider a solution displaying Dirac nodes: $\vec{u}_1 = |\vec{u}_1|(1,0,0)^T, \vec{u}_2 = |\vec{u}_1|(0,1,0)^T$ (all other variational parameters vanish). Amongst the trial solutions, this solution is lowest in energy, see Tab. I, third row. It corresponds to a p + ip superconductor of spinons, which is nothing but $|BCS:p_x + ip_y\rangle$ as presented in Eq. (9b). Note that the choice of a homogeneous λ only respects the constraint of half filled sites on average. To impose the Gutzwiller projection on each site amounts to careful integration over gauge field fluctuations which is beyond the scope of this work.

Triangular lattice

Next, we repeat the same analysis for the triangular lattice, for which Eq. (20) holds equally, yet with z = 6 (and therefore three sets of order parameter fields $\kappa'_{l=1,2,3}, \vec{u}_{l=1,2,3})$ and $\hat{e}_1 = (1,0)^T, \hat{e}_2 = (1,\sqrt{3})^T/2, \hat{e}_3 =$ $(-1,\sqrt{3})^T/2$, see Fig. 3 b). The mean-field solutions are displayed in the right column of Tab. I. First, consider $\kappa_1' = \kappa_2' = \kappa_3' > 0$, for which half-filling

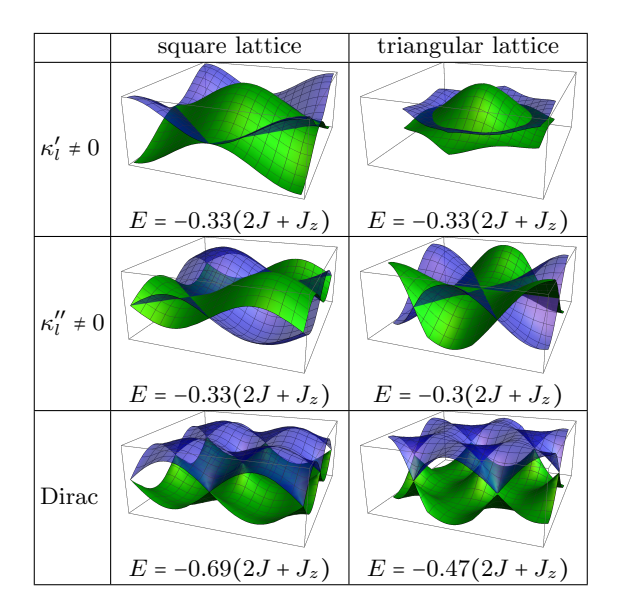


TABLE I. Illustration of spinon dispersion in the first Brillouin zone and estimate of the ground state energy (per site) for selected trial mean-field solutions on square and triangular lattices, as discussed in Secs. III A,III B. The Dirac solution is $\vec{u}_1 \perp \vec{u}_2 \perp \vec{u}_3$ ($\vec{u}_1 \perp \vec{u}_2$) on the triangular (square) lattice. For comparison, the energy of the ferromagnetic in plane solution is -3J (-2J) for triangular (square lattice).

implies $\lambda = -0.836\kappa'_1$. This state displays a Fermi surface and is C_6 invariant.

As a second normal state solution we consider $\kappa_l'' = -|\kappa_1''|(-1)^l$, while all other parameters $\kappa_l' = \Delta_l' = \Delta_l'' = \lambda = 0$. Note that a flux $\pi/2$ $(-\pi/2)$ is enclosed in downside (upside) triangles. Contrary to the case of the square lattice, this state is thus not gauge equivalent to the state with real hopping. On the other hand, a variety of superconducting solutions $\kappa_l' = \kappa_l'' = 0$, $|\Delta_l| \neq 0$ are equivalent by SU(2) isospin symmetry.

Finally, we consider a solution displaying Dirac nodes: $\vec{u}_1 = |\vec{u}_1|(1,0,0)^T, \vec{u}_2 = |\vec{u}_1|(0,1,0)^T, \vec{u}_3 = |\vec{u}_1|(0,0,1)^T$ (all other variational parameters vanish). As for the square lattice, this solution is lowest in energy and corresponds to a p+ip superconductor of spinons. In the next section, we demonstrate on the basis of a microscopically derived Ginzburg-Landau function, that the Dirac QSL establishes as the dominant instability at finite temperature.

C. Finite temperature transition and doping

We here consider the finite temperature transition and the effect of doping on the mean field spinon solution treating square and triangular lattices in parallel. This leads to the phase diagram presented in Fig. 1 c. In the calculation we distinguish two regimes: the limit of a degenerate Fermi gas $t_f \gg T$ and the reverse high temperature limit $t_f \ll T$.

We anticipate the result of Sec. IIIE that $t_f = \delta t$ in

all relevant regimes and that the degenerate Fermi gas (high temperature classical gas) limit is important for the finite temperature transition at large (small) doping $\delta \gg |E_{\rm VB}|/t$ ($\delta \ll |E_{\rm VB}|/t$), see end of this section.

The integration of fermions leads to the following free energy density

$$F = -\frac{T}{2\mathcal{A}} \sum_{n} \sum_{\mathbf{k}} \operatorname{tr} \ln[i\epsilon_n - h(\mathbf{k})] + \frac{2}{|E_{\text{tVB}}|} \sum_{l=1}^{z/2} (\kappa_l^{\prime 2} + |\vec{u}_l|^2).$$
(21)

Here, \mathcal{A} is the total number of sites (i.e. the system size). The expansion of the fermionic determinant in small order parameter fields leads to a Ginzburg-Landau functional (see Appendix A 2)

$$F = \sum_{l=1}^{z/2} \left[A_{+} \vec{u}_{l}^{T} \vec{u}_{l} - A_{-} \vec{u}_{l}^{T} \begin{pmatrix} 1 & 0 & 0 \\ 0 & 1 & 0 \\ 0 & 0 & -1 \end{pmatrix} \vec{u}_{l} + C |\vec{u}_{l}|^{4} \right] + \frac{D}{2} \sum_{l,l'=1}^{z/2} \left[\vec{u}_{l}^{2} \vec{u}_{l'}^{2} + 2 (\vec{u}_{l} \cdot \vec{u}_{l'})^{2} \right].$$
(22)

Here, we disregarded κ' , which has a subdominant critical temperature in both limits $t_f \ll T$ and $t_f \gg T$. We also emphasize that the constraint field λ does not couple linearly to any of the order parameter fields, this is evident from the matrix structure of $h(\mathbf{k})$, Eq. (20b).

It is worthwhile to point out the main difference to conventional RVB theory, namely the absence of a linear symmetry breaking term of the kind $\delta F_{\rm RVB} \propto -(0,0,1) \sum_l \vec{u}_l$. This is a consequence of the different matrix structure in spin space of the order parameter fields, i.e. presence of σ_z in the decoupled terms in Eq. (18). At any finite δ , the isospin SU(2) symmetry is broken by the A_- term.

We first qualitatively discuss the mean field solutions assuming C=0, $A_-\geq 0$ and $A_+ \propto T-T_{\rm tRVB}$, where $T_{\rm tRVB}$ is the mean field transition temperature. In the important parameter regime, these assumptions are consistent with the microscopically derived values presented at the end of this section.

The quartic term with a scalar product is crucial in discriminating the lowest energy state and favors \vec{u}_l which are perpendicular on different bonds $l=1,\ldots,z/2$ of the unit cell. This reproduces analogous results of singlet RVB theory on the square lattice, which we reviewed in Sec. IIB. In contrast to singlet RVB theory, however, the quadratic anisotropy term A_- favors easy plane solutions in which the superconducting components of $\vec{u}_l = (\Delta_l', \Delta_l'', \kappa_l'')$ are dominant. More specifically, for the triangular lattice, the mean field order parameter is $\vec{u}_l \propto ((-1)^l \hat{e}_l^T, u_z)^T$, where $u_z = \sqrt{1-3A_-}/\sqrt{4A_-+2}$ interpolates between the Dirac solution, Tab. I lowest row, and a p-wave superconducting solution with complex nearest neighbor pairing $\Delta_l \propto e^{i2\pi l/3}$ and $\kappa_l'' = 0$. In the case of the square lattice, where the coordination number z is smaller, the p-wave superconducting solution

is the ground state for any A_- . In this case $\Delta_l \propto e^{i\pi l/2}$ and $\kappa_l'' = 0$.

We proceed with a discussion of microscopic values of the Ginzburg-Landau parameters. In the high temperature regime $t_f \ll T$, we find $A_- \sim t_f^2/T^3 > 0$, C = 0, $D \sim T^{-3}$ and $A_+ \sim [T - T_{\rm tRVB}]/T^2$ with $T_{\rm tRVB} \simeq |E_{\rm tVB}|/4$. Using $t_f = \delta t$, we find that the regime $t_f \ll T$ is relevant to the finite temperature transition at low doping, $\delta \ll |E_{\rm VB}|/t$. The emergent SO(3) symmetry at $A_- \propto t_f^2 \to 0$ ($\vec{u}_l \to O\vec{u}_l$) reflects the SU(2) invariance in Nambu space in Eq. (20b). This SU(2) symmetry is weakly broken in the regime of weak doping $0 < t_f/T \ll 1$ which, as mentioned, favors the superconducting state.

This tendency is strongly reinforced in the complementary regime of the degenerate electron gas $t_f \gg T$, because $A_+ - A_-$ develops a logarithmic Cooper instability while all other constants remain finite (note that in this case generically $C \neq 0$). In this limit, the mean field transition temperature $T_{\rm tRVB} \sim t_f e^{-\mathcal{C}t_f/|E_{\rm tVB}|}$ where we estimate $\mathcal{C} \simeq 16\pi\sqrt{3}$ ($\mathcal{C} \simeq 16\pi$) for triangular (square) lattice in the continuum limit. Using again $t_f = \delta t$, the degenerate electron gas assumption applies to the finite temperature transition at strong doping $\delta \gg |E_{\rm tVB}|/t$. In Fig. 1 c we present an interpolation of the mean field transition temperature which captures both regimes $\delta \ll |E_{\rm tVB}|/t$ and $\delta \gg |E_{\rm tVB}|/t$.

D. Observables

We emphasize that the mean field solutions, which are characterized by $\kappa' = 0$, do not display a finite magnetization $\vec{m} = T \sum_{n,\mathbf{k}} \operatorname{tr}[\vec{\sigma}\mathcal{G}_{n,\mathbf{k}}]$, as can be readily seen from the matrix structure of $\mathcal{G}_{n,\mathbf{k}}^{-1} = i\epsilon_n - h(\mathbf{k})$. At the same time, short range magnetic correlations are key observables and reflected in the dynamical structure factor, Fig. 2. We here explain its characteristic features using the selection rules implied by the mean field Hamiltonian of Abrikosov fermions, Fig. 4. Both RVB and tRVB Hamiltonians are characterized by a direct product of a momentum dependent matrix in Nambu space and a matrix in spin space which is unity in the case of RVB and σ_z for tRVB. At each momentum \mathbf{k} , we denote the eigenstate with positive (negative) eigenvalue of the matrix in Nambu space by $|+\rangle$ $(|-\rangle)$. Hence, at each \mathbf{k} , $|-\rangle \otimes |\uparrow\rangle$, $|-\rangle \otimes |\downarrow\rangle$ are the negative energy states of $h_{\text{RVB}}(\mathbf{k})$, and positive energy states are $|+\rangle \otimes |\uparrow\rangle, |+\rangle \otimes |\downarrow\rangle$. Thus, the matrix element for vertical spin flip transitions vanishes and the dynamical structure factor is suppressed at zero momentum transfer, $\mathbf{Q} = 0$, see Fig. 2 c). For the square lattice, $h_{\text{RVB}}(\mathbf{k}) = -h_{\text{RVB}}(\mathbf{k} + \mathbf{Q}_{\text{N\'eel}})$ and spin flip matrix elements at momentum difference $\mathbf{Q}_{\mathrm{N\acute{e}el}}$ = (π,π) are maximents mal and by consequence the structure factor is dominated by the Néel wave vector, green arrow in Fig. 4 a). In contrast, for $h_{\text{tRVB}}(\mathbf{k})$, $|-\rangle \otimes |\uparrow\rangle$ and $|+\rangle \otimes |\downarrow\rangle$ are the negative energy states, their spin-flip matrix element with positive energy states $|-\rangle \otimes |\downarrow\rangle$ and $|+\rangle \otimes |\uparrow\rangle$ is finite and vertical

transitions are therefore allowed, Fig. 4 b). This leads to a predominantly ferromagnetic spin fluctuation spectrum, Fig. 2 d).

E. Bosonic Hamiltonian and BKT transition

So far, we have ignored the slave bosons and simply replaced $t\langle b_i b_j^{\dagger} \rangle \to t_f$ in Eq. (18). In this short section, we reverse the situation and study the bosonic part of Eq. (18) under the replacement $t \sum_{\sigma} \langle f_{i,\sigma} f_{j,\sigma}^{\dagger} \rangle \to t_b$.

We consider the low-density limit, for which the 2D Bose gas is described by the continuum action

$$S = \int d\tau d^2x \bar{\psi} \left[\partial_{\tau} - \mu_{\text{eff}} - \frac{\nabla^2}{2m} \right] \psi + \frac{g}{2} |\psi|^4.$$
 (23)

2D Bose-Einstein condensation is known to be absent in the non-interacting limit and driven by the confinement of topological defects, otherwise. The Berezinskii-Kosterlitz-Thouless transition temperature which captures these aspects in the limit $mg \ll 1$ is 61

$$T_{\text{BKT}} = \frac{2\pi}{m} \frac{n}{\ln\left(\frac{380}{mq}\right)},\tag{24}$$

where n is the density in the continuum limit.

The mapping between the lattice Hamiltonian and the continuum theory as well as microscopic values for the parameters of the action (23) are contained in App. C and lead to a non-trivial relationship between mg and V/t_b , see Fig. 5. We exploit this as we push Eq. (24) to the limit of its applicability at $mg \sim 1$ using

$$T_{\text{BKT}} = \frac{2\pi z t_b \delta}{\ln[95(1 + 2z t_b/V)/z]}$$
 (25)

to interpolate between weak and strong coupling.

F. Self-consistency of hopping amplitudes

We now present estimates for t_f and t_b as a function of external parameters $\delta, E_{\text{tVB}}, t$ and first summarize our results:

For the entire relevant parameter regime, $t_f = \delta t$ while t_b has a different form in weak doping regime $\delta < |E_{\rm tVB}|/t \ll 1$ and strong doping regime $|E_{\rm tVB}|/t < \delta$. In the weak doping regime, $t_b \sim \delta t^2/|E_{\rm tVB}|$ and in the strong doping regime $t_b \sim (1-\delta)t$. For a pictorial summary of these results and associated regimes, see Fig. 6. Formally, the results for the BKT transition in the weak doping regime are valid for $T \ll t_b$, while for the BCS like transition at strong doping we require $T \ll t_f$. Both $T_{\rm tRVB}$, $T_{\rm BKT}$ satisfy these bounds (we assume $V \sim |E_{\rm tVB}|$), see also Fig. 1 c.

To derive these results, we first concentrate on the limit $t_f \ll \max_l |\vec{u}_l|$. It is important to emphasize that,

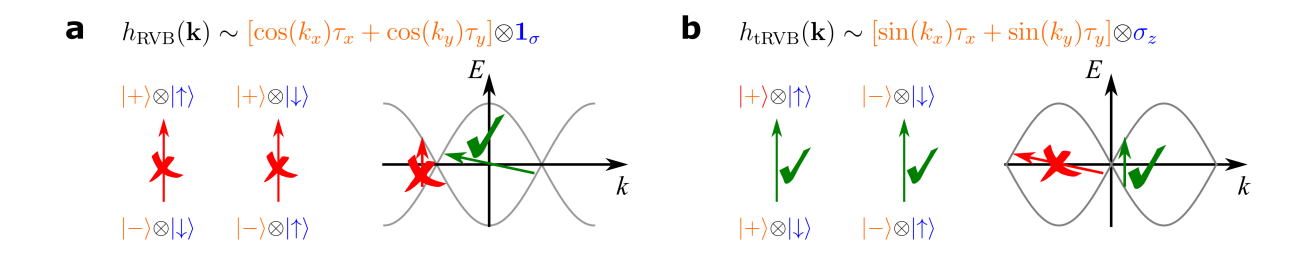


FIG. 4. Selection rules for the dynamical structure factor for a) the RVB state and b) the tRVB state on the square lattice. For further explanations, see main text.

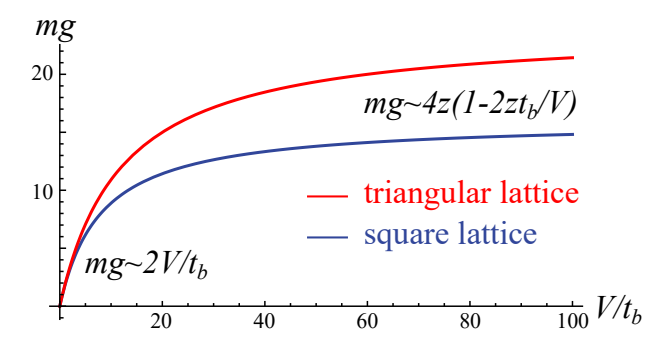


FIG. 5. The dimensionless parameter mg entering Eqs. (23),(24) as a function of microscopic parameters of the bosonic theory Eq. (18).

contrary to usual singlet RVB theory, ¹² magnetic interactions do not contribute to the fermion hopping term proportional to t_f , see Eq. (20b). Therefore (assuming nearest neighbors i and j),

$$t_b = t \sum_{\sigma} \langle f_{i,\sigma}^{\dagger} f_{j,\sigma} \rangle \simeq \frac{2Tt}{\mathcal{A}} \sum_{\mathbf{k},n} \frac{-\xi_{\mathbf{k}} e^{i\mathbf{k} \cdot (\mathbf{x}_i - \mathbf{x}_j)}}{\epsilon_n^2 + |\sum_l \vec{u}_l \sin(\mathbf{k} \cdot \hat{e}_l)|^2}$$
(26)

Without going into details, we conclude that $t_b \sim t_f t/|E_{\text{tVB}}| > 0$ at temperatures far below T_{tRVB} .

On the other hand, in the limit of dominant normal hopping, $t_f \gg \max_l |\vec{u}_l|$, one may omit the mean field order parameter in the evaluation of $t_b = t \sum_{\sigma} \langle f_{i,\sigma}^{\dagger} f_{j,\sigma} \rangle \simeq t(1-\delta)$. The approximate replacement of the fermionic correlator by the fermion density $1-\delta$ becomes exact in the continuum limit.

Finally, we consider $t_f = t \sum_{\sigma} \langle b_j^{\dagger} b_i \rangle$. It is obvious that $t_f = \delta t$ in the superfluid, where $\langle b_i \rangle = \sqrt{\delta} e^{i\phi_i}$. We now show that $t_f = \delta t$ also in the normal state and exploit that the relevant regime regards low densities. In this limit the bosonic Hamiltonian can be linearized, $H = \sum_{\mathbf{k}} b_{\mathbf{k}}^{\dagger} \xi_{\mathbf{k}}^{b} b_{\mathbf{k}}$, where $\xi_{\mathbf{k}}^{b}$ has a minimum at $\mathbf{k} = 0$ and bandwidth t_b . Then

$$t_f \simeq \frac{t}{\mathcal{A}} \sum_{\mathbf{k}} e^{i\mathbf{k}\cdot(\mathbf{x}_i - \mathbf{x}_j)} n_{\text{BE}}(\xi_{\mathbf{k}}^b) \simeq \delta t.$$
 (27)

Here $n_{\text{BE}}(\xi_{\mathbf{k}}^b)$ is the Bose-Einstein distribution. At the second asymptotic equality sign, we have used the con-

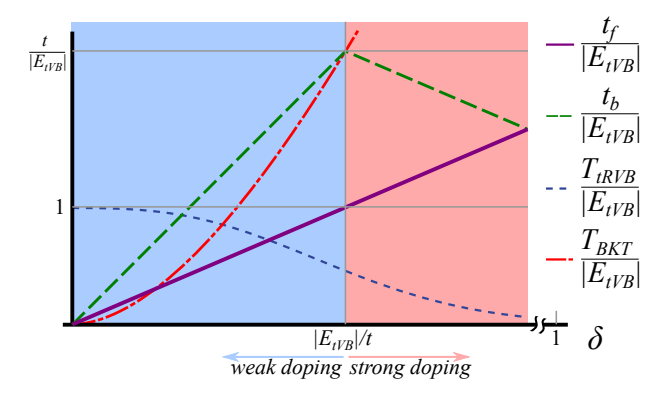


FIG. 6. Estimated relationship between internal parameters t_b, t_f and external parameters δ, t, E_{tVB} (note $t \gg |E_{tVB}|$ is assumed).

tinuum limit (expansion about $\mathbf{k}=0$), which is justified for temperatures $T\ll t_b$.

We conclude with a remark that the discrimination of two regimes $t_f \ll \max_l |\vec{u}_l|$, $t_f \gg \max_l |\vec{u}_l|$ at temperatures far below $T_{\rm tRVB}$ is equivalent to $\delta t \ll |E_{\rm tVB}|$, $\delta t \gg |E_{\rm tVB}|$, respectively.

IV. CONCLUSION

In summary, we have studied tRVB states on 2D triangular and square lattices using an Abrikosov fermion mean field treatment of an anisotropic nearest neighbor ferromagnetic Heisenberg model. We found a gapless Dirac spin liquid for either lattice. We furthermore studied the effect of doping away from the Mott insulator limit and thereby discovered a novel mechanism for the appearance of p+ip triplet superconductivity.

We conclude with an outlook. On the abstract theoretical side, a question about the stability of the tRVB mean field solutions arises for spin 1/2 Hamiltonians. To appreciate the exigency of this question for the present ferromagnetic model Eq. (10), it is instructive to recapitulate what is known about the analogous question for the SU(2) invariant quantum antiferromagnet. For the latter, neither triangular nor square lattices display a spin-liquid ground state (but rather 120° collinear

and Néel antiferromagnetism), despite the fact that the mean field Abrikosov-fermion treatment yields Dirac spin-liquids. 8,12,50 In the present, predominantly ferromagnetic case, the situation is likely similar, and indeed the in-plane ferromagnetic solution with energy -3J(-2J) is lower than any of the tRVB trial states of table I in a substantial fraction of the parameter regime. Therefore, it is an important task for the future to find an easy plane (U(1) spin symmetric) ferromagnetic spin-1/2 Hamiltonian including longer-range and multi-spin interactions which rigorously displays a tRVB ground state and to study when it is of the Dirac or of the spinon Fermi surface type represented in Tab. I. Since tRVB states do not have any minus signs, a Quantum Monte Carlo simulation would be a promising route for such study. Given the variety of physical states which can be encoded by RVB trial states with different bond lengths and which include ordered magnets and \mathbb{Z}_2 as well as U(1) QSLs, 45,62,63 it is also an interesting task to study longer range tRVB trial states.

Regarding the concrete material 1T-TaS₂ (and related monolayer TaSe₂, NbSe₂), reliable understanding about the scale and sign of the exchange interactions is necessary, both experimentally and theoretically. Here we have presented a theory which displays quantum spinliquid behavior, even when the exchange interactions are predominantly ferromagnetic. A spinon Fermi surface either from singlet or triplet RVB could potentially account for linear temperature scaling in specific heat and thermal conductivity. However, the lowest state within our mean-field approach is a tRVB QSL with Fermi points and Dirac excitations. While the mean-field solutions with a spinon Fermi surface have higher energy, they might be stabilized by certain longer-range interactions. Incidentally, within our theory, doping leads to a time reversal symmetry breaking superconductor which is indeed believed to be observed in stacked multilayers of 1T-TaS₂ and metallic 1H-TaS₂. ³³ On the other hand, if present estimates of exchange interactions on the order of a few Kelvin are correct, an alternative to the theoretical QSL explanation for the weak Curie-Weiss signal appears inevitable.

Beyond the issue of 1T-TaS₂, our proposal opens room for a new and exciting experimental and numerical search for QSLs and topological order in local moment systems with predominantly ferromagnetic coupling that do not order down to very low temperatures.

V. ACKNOWLEDGMENTS

It is a pleasure to acknowledge useful discussions with L. Classen, B. Jäck and D. Pasquier.

This work was supported by the U.S. Department of Energy, Office of Basic Energy Sciences, under Contract No. DE-FG02-99ER45790 (E.J.K., P.C.), the National Science Foundation Grant No. DMR-1830707 (Y.K.) and was completed at the Aspen Center for Physics, which is

supported by National Science Foundation grant PHY- 1607611.

APPENDIX

Appendix A: Mean field slave boson theory for SU(2)

In this appendix we provide details on our calculations of a $t\!-\!J$ model with anisotropic, ferromagnetic exchange interaction.

1. Attractive interaction channels

The spinon interaction in Eq. (11) contains intersite interaction of singlet particle-hole $f_i^{\dagger}f_j$ and particle-particle $f_i^{\dagger}\sigma_y f_j^{\dagger}$ and of triplet m_z = 0 particle-hole $f_i^{\dagger}\sigma_z f_j$ and particle-particle $f_i^{\dagger}\sigma_x f_j^{\dagger}$ operators. We drop the interaction of repulsive interaction channels of triplet m_z = ±1 operators and obtain

$$H_{J} = \sum_{\langle i,j \rangle} \frac{1}{2} \Big[E_{\text{sVB}}(f_{i}^{\dagger} f_{j}) (f_{j}^{\dagger} f_{i}) + E_{\text{tVB}}(f_{i}^{\dagger} \sigma_{z} f_{j}) (f_{j}^{\dagger} \sigma_{z} f_{i}) + E_{\text{tVB}}(f_{i}^{\dagger} \sigma_{x} f_{j}^{\dagger}) (f_{j} \sigma_{x} f_{i}) + E_{\text{sVB}}(f_{i}^{\dagger} \sigma_{y} f_{j}^{\dagger}) (f_{j} \sigma_{y} f_{i}) \Big].$$
(A1)

Since we are interested in the regime $E_{\text{tVB}} < E_{\text{sVB}}$ and $E_{\text{tVB}} < 0$, we decouple only the second and third line in Eq. (18) of the main text.

2. Free energy expansion

We expand the fermionic contribution to the free energy density, Eq. (21), in powers of κ', \vec{u} .

The zeroth order is given by

$$F_0 = 2\frac{T}{\mathcal{A}} \sum_{\mathbf{k}} \ln(1 + e^{-\xi_{\mathbf{k}}/T}), \tag{A2}$$

while higher order contributions are formally

$$\Delta F = -\frac{T}{2\mathcal{A}} \sum_{n,\mathbf{k}} \operatorname{tr}^{\sigma,\tau} \ln[\mathbf{1} - \mathcal{G}_{n,\mathbf{k}}^{(0)} \delta h_{\mathbf{k}}]$$

$$\simeq \frac{T}{2\mathcal{A}} \sum_{n,\mathbf{k}} \left(\frac{1}{2} \operatorname{tr}^{\sigma,\tau} \left[(\mathcal{G}_{n,\mathbf{k}}^{(0)} \delta h_{\mathbf{k}})^{2} \right] + \frac{1}{4} \operatorname{tr}^{\sigma,\tau} \left[(\mathcal{G}_{n,\mathbf{k}}^{(0)} \delta h_{\mathbf{k}})^{4} \right] \right). \tag{A3}$$

Here
$$\mathcal{G}_{n,\mathbf{k}} = \begin{pmatrix} G_{n,\mathbf{k}} & 0 \\ 0 & -\bar{G}_{n,\mathbf{k}} \end{pmatrix}$$
 and $G_{n,\mathbf{k}} = (i\epsilon_n - \xi_{\mathbf{k}})^{-1}$. All terms with odd powers in the series expansion vanish by spin summation. This is in contrast to usual singlet RVB theory, where there is a linear term $\Delta F \sim -t_f \sum_l \kappa_l'$.

a. Second order term

We introduce the three integrals

$$A_{\pm}^{(ll')} = \frac{T}{\mathcal{A}} \sum_{n,\mathbf{k}} \sin(k_l) \sin(k_{l'}) \left(\frac{1}{i\epsilon_n - \xi_{\mathbf{k}}} \pm \frac{1}{i\epsilon_n + \xi_{\mathbf{k}}} \right)^2$$

$$= -\frac{1}{\mathcal{A}} \sum_{\mathbf{k}} \sin(k_l) \sin(k_{l'})$$

$$\times \left\{ \frac{1}{2T[\cosh(\xi_{\mathbf{k}}/[2T])]^2} \pm \frac{\tanh(\xi_{\mathbf{k}}/[2T])}{\xi_{\mathbf{k}}} \right\}, (A4a)$$

$$B^{(ll')} = \frac{T}{\mathcal{A}} \sum_{n,\mathbf{k}} \cos(k_l) \cos(k_{l'}) \left(\frac{1}{(i\epsilon_n - \xi_{\mathbf{k}})^2} + \frac{1}{(i\epsilon_n + \xi_{\mathbf{k}})^2} \right)$$

$$= -\frac{1}{2T\mathcal{A}} \sum_{\mathbf{k}} \frac{\cos(k_l) \cos(k_{l'})}{[\cosh(\xi_{\mathbf{k}}/[2T])]^2}. \tag{A4b}$$

Using this integrals we obtain after traces in Nambu and spin space (Einstein summations to be understood)

$$F_{2} = A_{+}^{(ll')} \vec{u}_{l} \cdot \vec{u}_{l'} - A_{-}^{(ll')} \vec{u}_{l}^{T} \begin{pmatrix} 1 & 0 & 0 \\ 0 & 1 & 0 \\ 0 & 0 & -1 \end{pmatrix} \vec{u}_{l'} + 2B^{(ll')} \kappa_{l}' \kappa_{l'}'. \tag{A5}$$

In Eq. (21) of the main text we slightly abuse our notations and absorb $A_{+}^{(ll')} + 2\delta_{ll'}/|E_{\text{tVB}}| \to A_{+}^{(ll')}$

b. Mean field instabilities

We first consider the regime $t_f = \delta t \ll T \ll t$. In this limit, $\partial f/\partial \lambda = 0$ leads to $\lambda \approx 2\delta T \ll t_f$. Expansion in $\xi_{\bf k} \ll T$ leads to

$$A_{+}^{ll'} \simeq -\frac{1}{T\mathcal{A}} \sum_{\mathbf{k}} \sin(k_{l}) \sin(k'_{l}) \left(1 - \xi_{\mathbf{k}}^{2}/6\right)$$

$$\simeq -\frac{\delta_{ll'}}{2T} \begin{cases} \left[1 - \frac{5}{6} \left(\frac{t_{f}}{T}\right)^{2}\right], & \text{triangular latt.,} \\ 1 - \frac{3}{6} \left(\frac{t_{f}}{T}\right)^{2}\right], & \text{square latt.,} \end{cases}$$

$$A_{-}^{ll'} \simeq \frac{1}{T\mathcal{A}} \sum_{\mathbf{k}} \sin(k_{l}) \sin(k'_{l}) \xi_{\mathbf{k}}^{2}/12$$

$$\simeq \frac{\delta_{ll'}}{24T} \begin{cases} \left[5 \left(\frac{t_{f}}{T}\right)^{2}\right], & \text{triangular latt.,} \\ 3 \left(\frac{t_{f}}{T}\right)^{2}\right], & \text{square latt.,} \end{cases}$$

$$B \simeq -\frac{1}{2T\mathcal{A}} \sum_{\mathbf{k}} \cos(k_{l}) \cos(k'_{l}) (1 - \xi_{\mathbf{k}}^{2}/4)$$

$$\simeq -\frac{1}{4T} \begin{cases} \left[1 - \frac{1}{4} \left(\frac{t_{f}}{T}\right)^{2} \left(\frac{7}{2} \cdot \frac{2}{2} \cdot \frac{2}{2} \cdot \frac{2}{7} \cdot \frac$$

The largest transition temperature T_c is thus associated to the order parameter Δ_l', Δ_l'' with T_c = $|E_{\rm tVB}|/4(1$ –

 $20(t_f/|E_{\text{tVB}}|)^2/3)$ [$T_c = |E_{\text{tVB}}|/4(1 - 5(t_f/|E_{\text{tVB}}|)^2)$] for the triangular [square] lattice. The critical temperatures associated to κ are order $(t_f/J)^2$ times lower.

We now consider the regime $T \ll t_f$. A logarithmic Cooper instability in Eq. (A4), manifest through the typical momentum sum $\Sigma_{\bf k}$ tanh $[\xi_{\bf k}/(2T)]/\xi_{\bf k}$, only occurs for the combination $A_+^{(ll')} - A_-^{(ll')} \sim -\rho \delta_{ll'} \ln(t_f/T)$ (right at a van-Hove singularity, other terms may also have logarithmic coefficients). Here we employed t_f as the UV cut-off of our theory and we introduced the density of states ρ which in the simplified, parabolic limit obtained by expansion of the dispersion about the Γ point is $\rho = 1/(8\sqrt{3}\pi t_f)$ [$\rho = 1/(8\pi t_f)$] for triangular [square] lattice. Clearly, the parabolic approximation is considerably better for the triangular lattice which does not display a van-Hove singularity at half-filling.

We observe that κ' does not develop a (dominant) mean field instability in either $T \ll t_f$ nor $t_f \ll T \ll t$. It will therefore be omitted in the following and is not included in Eq. (22) of the main text.

c. Fourth order term

We obtain the following expansion of the trace

$$\operatorname{tr}^{\sigma\tau} \left[\left(\mathcal{G}\vec{h} \cdot \vec{\tau} \sigma_z \right)^4 \right] / 2 = 2|G|^4 \vec{h}^4 - 4|G|^2 (G + \bar{G})^2 (h_1^2 + h_2^2) h_3^2 + (G^2 - \bar{G}^2)^2 h_3^4.$$
 (A9)

Here, we have omitted the subscript n, \mathbf{k} of the Green's functions, and $\vec{h} = \vec{h}(\mathbf{k}) = 2 \sum_{l} \vec{u}_{l} \sin(k_{l})$.

We keep only the first line $2|G|^4\bar{h}^4$ of Eq. (A9). In the limit of small $t_f \ll T$ this is justified, since the terms of the second and third line vanish (this is a manifestation of the SU(2) symmetry). In the opposite limit, $t_f \gg T$ the leading, quadratic instability regards superconducting order parameters $\Delta_l' \Delta_l''$, only, and we can disregard the additional corrections from h_3 terms.

In summary, this motivates us to drop SU(2) breaking terms from the quartic term. The relevant integrals in the derivation of quartic terms are thus

$$I_{\{k_i\}} = \frac{2T}{\mathcal{A}} \sum_{n,\mathbf{k}} |G_{n,\mathbf{k}}|^4 \prod_{i=1}^4 \sin(k_{l_i}).$$
 (A10)

By mirror symmetry $k_1 \rightarrow -k_1$, the only non-zero integrals have either all l_i equal, or l_i pairwise equal. By rotational symmetry, all non-zero integrals can thus be

expressed as one of the following integrals

$$\tilde{C} = \frac{2T}{A} \sum_{n,\mathbf{k}} |G_{n,\mathbf{k}}|^4 \sin(k_1)^4$$

$$= \frac{7\zeta(3)}{4\pi^2 T^3} \frac{1}{A} \sum_{\mathbf{k}} f(\xi_{\mathbf{k}}/T) \sin(k_1)^4, \qquad (A11a)$$

$$D = \frac{4T}{A} \sum_{n,\mathbf{k}} |G_{n,\mathbf{k}}|^4 \sin(k_1)^2 \sin(k_2)^2$$

$$= \frac{7\zeta(3)}{4\pi^2 T^3} \frac{2}{A} \sum_{\mathbf{k}} f(\xi_{\mathbf{k}}/T) \sin(k_1)^2 \sin(k_2)^2. (A11b)$$

Here, $f(x) = -\pi^2(x - \sinh(x)) \operatorname{sech}^2(x/2)/(7\zeta(3)x^3)$ (which is normalized to $\int dx f(x) = 1$) places the integrals on the Fermi surface.

In the regimes of interest we estimate these constant as follows: for $t_f \ll T \ll t, \ C, D \sim T^{-3} \sim J^{-3}$, while for $T \ll t_f, \ C, D \sim T^{-2}/[t_f] \sim J^{-2}/[t_f]$.

With this notation we obtain

$$F_4 = \sum_{l} \tilde{C} \vec{u}_l^4 + \frac{D}{2} \sum_{l \neq l'} \left[\vec{u}_l^2 \vec{u}_{l'}^2 + 2(\vec{u}_l \cdot \vec{u}_{l'})^2 \right]$$
 (A12)

as reported in Eq. (22) of the main text, where we use the notation $C = \tilde{C} - 3D/2$.

Appendix B: Large N treatment of tRVB spin liquid

In this appendix, we demonstrate that the triplet quantum spin liquid discussed in the main text can be stabilized in an appropriate large N limit. Here we concentrate on the Mott insulator (i.e. $\delta = 0$) and $J_z = J$. In this limit, Eq. (10) can be written as

$$H = J \sum_{(i,j)} \sum_{\mu=1}^{3} (\hat{\sigma}_{z}^{(i)} \hat{\sigma}_{\mu}^{(i)} \hat{\sigma}_{z}^{(i)}) \hat{\sigma}_{\mu}^{(j)}.$$
(B1)

The easy plane nature is captured by the unitary transformation $\hat{\sigma}_z^{(i)}\hat{\sigma}_\mu^{(i)}\hat{\sigma}_z^{(i)}$ on the *i*-site. Note that Eq. (B1) holds for triangular and square lattices, alike.

Here we introduce a generalization of the SU(2) = Sp(2) spin group to Sp(2N) and the large-N model is

$$H = \frac{J}{N/3 + 2/3} \sum_{(i,j)} \sum_{\mu=1}^{2N^2 + N} (\hat{\sigma}_z^{(i)} \hat{\sigma}_\mu^{(i)} \hat{\sigma}_z^{(i)}) \hat{\sigma}_\mu^{(j)}.$$
(B2)

The notion of $\hat{\sigma}_z$ operators on a given site i will become clear shortly and the prefactor is chosen for convenience. The symplectic group is special, as it allows for the notion of time-reversal symmetry and thereby for superconducting spinon mean field theories. ⁶⁴ This feature is manifest in the usual matrix definition of the generators of the group

$$\hat{\sigma}_{\mu} = -\hat{\sigma}_{y} \hat{\sigma}_{\mu}^{T} \hat{\sigma}_{y}, \tag{B3}$$

where $\hat{\sigma}_y = \begin{pmatrix} 0 & -i\mathbf{1}_N \\ i\mathbf{1}_N & 0 \end{pmatrix} \equiv \sigma_y \otimes \mathbf{1}_N$ (where $\mathbf{1}_N$ is the $N \times N$ identity matrix).

For the present purpose of anisotropic quantum magnetism, it is convenient to represent the generators of Sp(2N) as $\sigma_{x,y,z}\otimes S$ and $\mathbf{1}_2\otimes A$, in particular $\hat{\sigma}_{y,z}=\sigma_{y,z}\otimes \mathbf{1}_N$ in Eqs. (B2),(B3). Here, S (A) are symmetric (antisymmetric) $N\times N$ matrices, clearly this parametrization fulfills Eq. (B3) and the number of generators $3N(N+1)/2+N(N-1)/2=2N^2+N$ agrees with the dimension of the group. We can thus rewrite Eq. (B2) as

$$H = -\frac{J}{N/3 + 2/3} \sum_{\langle i,j \rangle} \left\{ \sum_{S} [(\sigma_x \otimes S)^{(i)} (\sigma_x \otimes S)^{(j)} + (\sigma_y \otimes S)^{(i)} (\sigma_y \otimes S)^{(j)} - (\sigma_z \otimes S)^{(i)} (\sigma_z \otimes S)^{(j)}] - \sum_{A} (\mathbf{1}_2 \otimes A)^{(i)} (\mathbf{1}_2 \otimes A)^{(j)} \right\}.$$
(B4)

This expression clearly reflects the easy plane ferromagnetism of the original XXZ spin-1/2 model Eq. (10) of the main text (here \sum_{S} sums over symmetric $N \times N$ matrices and analogously \sum_{A} sums over antisymmetric matrices).

We now represent the symplectic spins as

$$\hat{\sigma}_{\mu} \to f_{a,\sigma}^{\dagger} [\hat{\sigma}_{\mu}]_{aa'} f_{a,\sigma}. \tag{B5}$$

Here, we introduced 2N species $(\sigma = \uparrow, \downarrow, \alpha = 1...N)$ of Abrikosov fermions.

In this notation, Eq. (B4) becomes

$$H = \frac{J}{N/3 + 2/3} \sum_{\langle i,j \rangle} \sum_{\mu=1}^{2N^2 + N} (f_i^{\dagger} \hat{\sigma}_z \hat{\sigma}_{\mu} \hat{\sigma}_z f_i) (f_j^{\dagger} \hat{\sigma}_{\mu} f_j)$$

$$= -\frac{J}{2N/3 + 4/3} \sum_{\langle i,j \rangle} (f_i^{\dagger} \hat{\sigma}_z f_j) (f_j^{\dagger} \hat{\sigma}_z f_i)$$

$$-\frac{J}{2N/3 + 4/3} \sum_{\langle i,j \rangle} (f_i^{\dagger} \hat{\sigma}_z \hat{\sigma}_y f_j^*) (f_j^T \hat{\sigma}_y \hat{\sigma}_z f_i) \quad (B6)$$

In the second line we used the Fierz identity of generators of appropriately normalized generators of Sp(2N)

$$\sum_{\mu} \hat{\sigma}^{\mu}_{\alpha\beta} \sum_{\mu} \hat{\sigma}^{\mu}_{\gamma\delta} = \frac{1}{2} \left(\delta_{\alpha\delta} \delta_{\beta\gamma} - (\hat{\sigma}_y)_{\alpha\gamma} (\hat{\sigma}_y)_{\delta\beta} \right). \tag{B7}$$

In this equation we used a multi-index notation $\alpha = (\sigma, a)$ etc

Clearly, the interaction is invariant under local transformations which leave $f_i f_i^{\dagger} + \sigma_y f_i^* f_i^T \sigma_y$ invariant, which leads to a local SU(2) symmetry. ⁶⁴ Here we will not dwell on these subtleties, and rather exploit that the large N limit prescribes the pattern of decoupling that we employed in Eq. (18)

$$H = \sum_{\langle i,j \rangle} \{ (\kappa_{ij} f_i^{\dagger} \hat{\sigma}_z f_j + H.c.) + [\Delta_{ij} f_i^T (i \hat{\sigma}_y) \hat{\sigma}_z f_j + H.c.] \}$$
$$+ \frac{2N}{|E_{\text{tVB}}|} \sum_{\langle i,j \rangle} [|\kappa_{ij}|^2 + |\Delta_{ij}|^2]. \tag{B8}$$

We used $E_{\text{tVB}} = -3J$ in the present limit. Upon integration of the spinons, the overall free energy therefore acquires an additional linear proportionality to "color index" N, whereby the mean-field approximation becomes justified.

Before closing, we remark that our search of mean-field solution within the limited set of homogeneous $\kappa_{i,j}$, $\Delta_{i,j}$ is not controlled by the large N limit and deserves special attention in future studies of the problem.

In summary, in this appendix we have presented an Sp(2N) generalization of Eq. (10) which allows to analytically control the mean field treatment of tRVB theories. It is apparent that this representation of Sp(2N) is favorable for any anisotropic quantum magnet and the application to Kitaev-Heisenberg models is left to future publications. 65

Appendix C: BKT transition

Here we summarize the mapping of the bosonic part of the Eq. (18)

$$H_b = -t_b \sum_{\langle i,j \rangle} [b_i^{\dagger} b_j + H.c.] - \tilde{\mu} \sum_i b_i^{\dagger} b_i + V \sum_{\langle i,j \rangle} (b_i^{\dagger} b_i) (b_j^{\dagger} b_j)$$
(C1)

to the continuum model, Eq. (23) and thereby we derive $T_{\rm BKT}$. We assume a grand canonical ensemble and here use $\tilde{\mu} = \mu - 2zV - \lambda$ to denote the effective boson chemical potential. The microscopic values for the coupling constants of Eq. (23) is derived in this section and summarized in Tab. II.

In the weak coupling limit $t_b \gg V$ we can expand $\xi_{\mathbf{k}}^b = -2t_b \sum_l \cos(\mathbf{k} \cdot \hat{e}_l) \simeq (-z + \frac{z\mathbf{k}^2}{2})t_b$ near the bottom of the band and thus identify $\xi_0^b = -zt_b$ (which is absorbed in μ) and the mass $m = 1/(zt_ba^2)$. Then, Eq. (23) can be directly derived by replacing $b_i \to a\psi(\mathbf{x}_i)$, with a being the lattice constant.

For the regime is $t_b \ll V$, we expand in small order parameter field Ψ by decoupling the kinetic term (for details see Ref. 66)

$$H_{\rm kin} = \sum_{\mathbf{k}} b_{\mathbf{k}}^{\dagger} E(\mathbf{k}) b_{\mathbf{k}} \rightarrow \sum_{i} b_{i}^{\dagger} \Psi_{i} + \bar{\Psi}_{i} b_{i} - \sum_{k} \bar{\Psi}(\mathbf{k}) E(\mathbf{k})^{-1} \Psi(\mathbf{k}).$$
(C2)

In Eq. (C2), the term linear in Ψ will be treated as a perturbation to $H_b|_{t_b=0}$, in which local occupations n_i are good quantum numbers allowing to formally diagonalize the Hamiltonian. In particular, the state without any boson has energy 0, while $E_1 = -\tilde{\mu}$ is the energy of a single boson on a given site, while $E_V = 2E_1 + V$ is the energy of a pair of bosons at adjacent sites.

The continuum theory of bosons, Eq. (23), near $\mu_{\rm eff}$ = 0 describes a (Mott-) insulator to superfluid quantum phase transition, and we formally derive this theory approaching the transition from the disordered side with $\mu_{\rm eff}$ < 0 such that no bosons are in the system at the

	$t_b \gg V$	$t_b \ll V$
m	$1/(zt_ba^2)$	$1/(zt_ba^2)$
$\mu_{ ext{eff}}$	$\mu - 2zV - \lambda + zt_b$	$\mu - 2zV - \lambda + zt_b$
g	$2zVa^2$	$4z^2t_ba^2(1-2zt_b/V)$
$T_{ m BKT}$	$\frac{2\pi z t_b n a^2}{\ln(190t_b/V)}$	$\frac{2\pi z t_b n a^2}{\ln\left(95/(z-2z^2t_b/V)\right)}$

TABLE II. Coupling constants of the continuum field theory of 2D bosons Eq. (23) as obtained from the bosonic part of Eq. (18) (here, we explicitly restored the lattice constant a).

ground state. We then assume that the parameters $m, g, \mu_{\rm eff}$ are the same also on the ordered side of the transition (in the relevant regime $\mu_{\rm eff} \sim \delta g/a^2$ is small but positive) and at temperatures of order $T_{\rm BKT}$.

By assumption, the ground state of $H_b|_{t_b=0}$ is then given by all sites empty and the leading excitations are given by the 1- and 2- boson states discussed above. We obtain from integrating out the b_i -bosons ⁶⁷

$$S = \int d\tau \sum_{i} \frac{\bar{\Psi}_{i}(-1 + E_{1}\partial_{\tau})\Psi_{i}}{E_{1}} + 4 \int d\tau \sum_{\langle i,j \rangle} \frac{|\Psi_{i}|^{2}|\Psi_{j}|^{2}}{E_{1}^{2}} \left(\frac{1}{2E_{1}} - \frac{1}{E_{V}}\right).$$
 (C3)

The quadratic term is obtained by perturbative inclusion of the dynamics of a single boson in the system. The quartic term can be obtained in the same manner, but it is equivalent and easier to calculate perturbative corrections to the ground state energy of $H_b|_{t_b=0}$ in the presence of a constant Ψ . The parameters of Tab. II, third column, and Eq. (23) are then obtained by identifying $\Psi_i \to a\psi(\mathbf{x}_i)E_1$ for weakly spatially dependent fields.

Physically, the presented calculation can be interpreted as follows. First, consider creating a single boson in the system. It costs onsite energy $E_1 = -\tilde{\mu} > 0$, but gains kinetic energy up to zt_b as it travels through the system. Clearly, the physics of a single boson is approximately valid in the small density limit, too, thus the free part of Eq. (23) is equivalent for non-interacting, weakly interacting and strongly interacting particles. However, the free theory needs to be complemented by scattering between two bosonic waves when two bosons are close (i.e. the g term). This depends on the microscopic details of the interaction potential, in particular its strength, as presented in Fig. 5.

¹ P. W. Anderson, Materials Research Bulletin 8, 153 (1973).

² P. Fazekas and P. W. Anderson, Philosophical Magazine

- **30**, 423 (1974).
- ³ L. Savary and L. Balents, Reports on Progress in Physics 80, 016502 (2016).
- ⁴ J. Knolle and R. Moessner, Annual Review of Condensed Matter Physics 10, 451 (2019).
- ⁵ S. A. Kivelson, D. S. Rokhsar, and J. P. Sethna, Phys. Rev. B 35, 8865 (1987).
- ⁶ Z. Zhu and S. R. White, Phys. Rev. B **92**, 041105 (2015).
- W.-J. Hu, S.-S. Gong, W. Zhu, and D. N. Sheng, Phys. Rev. B 92, 140403 (2015).
- ⁸ Y. Iqbal, W.-J. Hu, R. Thomale, D. Poilblanc, and F. Becca, Phys. Rev. B **93**, 144411 (2016).
- ⁹ D. S. Rokhsar and S. A. Kivelson, Phys. Rev. Lett. **61**, 2376 (1988).
- ¹⁰ J. Cano and P. Fendley, Phys. Rev. Lett. **105**, 067205 (2010).
- ¹¹ P. W. Anderson, science **235**, 1196 (1987).
- ¹² G. Kotliar and J. Liu, Phys. Rev. B **38**, 5142 (1988).
- ¹³ V. Emery and S. Kivelson, Nature **374**, 434 (1995).
- ¹⁴ S. Sachdev, Reports on Progress in Physics 82, 014001 (2018).
- ¹⁵ È. J. König, P. Coleman, and A. M. Tsvelik, Phys. Rev. B **102**, 155143 (2020).
- ¹⁶ C. Proust and L. Taillefer, Annual Review of Condensed Matter Physics 10, 409 (2019).
- ¹⁷ K. T. Law and P. A. Lee, Proceedings of the National Academy of Sciences 114, 6996 (2017).
- ¹⁸ M. Kratochvilova, A. D. Hillier, A. R. Wildes, L. Wang, S.-W. Cheong, and J.-G. Park, npj Quantum Materials 2, 1 (2017).
- ¹⁹ S. Qiao, X. Li, N. Wang, W. Ruan, C. Ye, P. Cai, Z. Hao, H. Yao, X. Chen, J. Wu, Y. Wang, and Z. Liu, Phys. Rev. X 7, 041054 (2017).
- ²⁰ P. Fazekas and E. Tosatti, Philosophical Magazine B 39, 229 (1979).
- A. Ribak, I. Silber, C. Baines, K. Chashka, Z. Salman, Y. Dagan, and A. Kanigel, Phys. Rev. B 96, 195131 (2017).
- ²² H. Murayama, Y. Sato, T. Taniguchi, R. Kurihara, X. Z. Xing, W. Huang, S. Kasahara, Y. Kasahara, I. Kimchi, M. Yoshida, Y. Iwasa, Y. Mizukami, T. Shibauchi, M. Konczykowski, and Y. Matsuda, Phys. Rev. Research 2, 013099 (2020).
- ²³ I. Lutsyk, M. Rogala, P. Dabrowski, P. Krukowski, P. J. Kowalczyk, A. Busiakiewicz, D. A. Kowalczyk, E. Lacinska, J. Binder, N. Olszowska, M. Kopciuszynski, K. Szalowski, M. Gmitra, R. Stepniewski, M. Jalochowski, J. J. Kolodziej, A. Wysmolek, and Z. Klusek, Phys. Rev. B 98, 195425 (2018).
- ²⁴ M. Klanjsek, A. Zorko, J. Mravlje, Z. Jaglicić, P. K. Biswas, P. Prelovsek, D. Mihailovic, D. Arcon, et al., Nature Physics 13, 1130 (2017).
- W. Ruan, Y. Chen, S. Tang, J. Hwang, H.-Z. Tsai, R. L. Lee, M. Wu, H. Ryu, S. Kahn, F. Liou, et al., Nature Physics (2021).
- ²⁶ W.-Y. He, X. Y. Xu, G. Chen, K. T. Law, and P. A. Lee, Phys. Rev. Lett. **121**, 046401 (2018).
- ²⁷ X.-L. Yu, D.-Y. Liu, Y.-M. Quan, J. Wu, H.-Q. Lin, K. Chang, and L.-J. Zou, Phys. Rev. B **96**, 125138 (2017).
- ²⁸ D. Pasquier and O. V. Yazyev, Phys. Rev. B **98**, 045114 (2018).
- ²⁹ M. Calandra, Phys. Rev. Lett. **121**, 026401 (2018).
- Y. Chen, W. Ruan, M. Wu, S. Tang, H. Ryu, H.-Z. Tsai, R. Lee, S. Kahn, F. Liou, C. Jia, et al., Nature Physics 16,

- 218 (2020).
- ³¹ The ferromagnetic exchange interaction of $J \sim 5K$ has been derived for monolayer 1T-NbSe₂. We are not aware of a similar derivation for bulk 1T-TaS₂, but expect a similar number from analogous techniques.
- ³² K. Rossnagel and N. V. Smith, Phys. Rev. B **73**, 073106 (2006).
- ³³ A. Ribak, R. M. Skiff, M. Mograbi, P. Rout, M. Fischer, J. Ruhman, K. Chashka, Y. Dagan, and A. Kanigel, Science advances 6, eaax9480 (2020).
- ³⁴ A. Ron, E. Zoghlin, L. Balents, S. D. Wilson, and D. Hsieh, Nature Communications **10** (2019), 10.1038/s41467-019-09663-3.
- M.-W. Lin, H. L. Zhuang, J. Yan, T. Z. Ward, A. A. Puretzky, C. M. Rouleau, Z. Gai, L. Liang, V. Meunier, B. G. Sumpter, P. Ganesh, P. R. C. Kent, D. B. Geohegan, D. G. Mandrus, and K. Xiao, Journal of Materials Chemistry C 4, 315 (2016).
- ³⁶ B. Liu, Y. Zou, L. Zhang, S. Zhou, Z. Wang, W. Wang, Z. Qu, and Y. Zhang, Scientific Reports 6 (2016), 10.1038/srep33873.
- ³⁷ J. Zhang, X. Cai, W. Xia, A. Liang, J. Huang, C. Wang, L. Yang, H. Yuan, Y. Chen, S. Zhang, Y. Guo, Z. Liu, and G. Li, Physical Review Letters 123, 047203 (2019).
- ³⁸ B. Siberchicot, S. Jobic, V. Carteaux, P. Gressier, and G. Ouvrard, The Journal of Physical Chemistry 100, 5863 (1996).
- ³⁹ T. J. Williams, A. A. Aczel, M. D. Lumsden, S. E. Nagler, M. B. Stone, J.-Q. Yan, and D. Mandrus, Physical Review B 92, 144404 (2015).
- W. Cai, H. Sun, W. Xia, C. Wu, Y. Liu, H. Liu, Y. Gong, D.-X. Yao, Y. Guo, and M. Wang, Physical Review B 102, 144525 (2020).
- ⁴¹ A. Kitaev, Annals of Physics **321**, 2 (2006).
- ⁴² B. Shen, Y. Zhang, Y. Komijani, M. Nicklas, R. Borth, A. Wang, Y. Chen, Z. Nie, R. Li, X. Lu, et al., Nature 579, 51 (2020).
- ⁴³ P. Coleman, Y. Komijani, and E. J. König, Phys. Rev. Lett. **125**, 077001 (2020).
- ⁴⁴ V. Drouin-Touchette, E. J. König, Y. Komijani, and P. Coleman, Phys. Rev. B **103**, 205147 (2021).
- ⁴⁵ A. F. Albuquerque, F. Alet, and R. Moessner, Phys. Rev. Lett. **109**, 147204 (2012).
- ⁴⁶ R. Moessner and S. L. Sondhi, Phys. Rev. Lett. **86**, 1881 (2001).
- ⁴⁷ P. Fendley, R. Moessner, and S. L. Sondhi, Phys. Rev. B 66, 214513 (2002).
- ⁴⁸ A. Ioselevich, D. A. Ivanov, and M. V. Feigelman, Phys. Rev. B **66**, 174405 (2002).
- ⁴⁹ P. Coleman, Phys. Rev. B **29**, 3035 (1984).
- ⁵⁰ I. Affleck and J. B. Marston, Phys. Rev. B **37**, 3774 (1988).
- ⁵¹ P. Coleman, Introduction to many-body physics (Cambridge University Press, 2015).
- ⁵² E. J. König, P. Coleman, and Y. Komijani, Phys. Rev. B 104, 115103 (2021).
- ⁵³ A. M. Polyakov, Nuclear Physics B **120**, 429 (1977).
- ⁵⁴ F. J. Wegner, Journal of Mathematical Physics **12**, 2259 (1971).
- ⁵⁵ T. Senthil and M. P. Fisher, Journal of Physics A: Mathematical and General 34, L119 (2001).
- M. Hermele, T. Senthil, M. P. A. Fisher, P. A. Lee, N. Nagaosa, and X.-G. Wen, Phys. Rev. B 70, 214437 (2004).
- ⁵⁷ A. E. Ruckenstein, P. J. Hirschfeld, and J. Appel, Phys. Rev. B **36**, 857 (1987).

- 58 P. A. Lee, N. Nagaosa, $\,$ and X.-G. Wen, Rev. Mod. Phys. **78**, 17 (2006).
- ⁵⁹ I. Affleck, Z. Zou, T. Hsu, and P. W. Anderson, Phys.
- Rev. B **38**, 745 (1988).

 S. Rachel, M. Laubach, J. Reuther, and R. Thomale, Phys. Rev. Lett. 114, 167201 (2015). N. Prokof'ev, O. Ruebenacker, and B. Svistunov, Phys.
- Rev. Lett. **87**, 270402 (2001).

 62 S. Liang, B. Doucot, and P. W. Anderson, Phys. Rev. Lett. 61, 365 (1988).
- ⁶³ J.-Y. Chen and D. Poilblanc, Phys. Rev. B **97**, 161107 (2018).
- ⁶⁴ R. Flint, M. Dzero, and P. Coleman, Nature Physics 4, 643 (2008).
- E. J. König *et al.*, Unpublished.
- 66 S. Sachdev, Quantum Phase Transitions (Cambridge University Press, 2011).
- 67 S. Saha, E. J. König, J. Lee, and J. H. Pixley, Phys. Rev. Research 2, 013252 (2020).